Folding and Stability of a Tryptophan-Containing Mutant of Ubiquitin

ARTICLE *in* BIOCHEMISTRY · AUGUST 1993

Impact Factor: 3.02 · DOI: 10.1021/bi00078a034 · Source: PubMed

Folding and Stability of a Tryptophan-Containing Mutant of Ubiquitin†

Sepideh Khorasanizadeh,‡,§ Iain D. Peters,‡ Tauseef R. Butt,∥,⊥ and Heinrich Roder*,‡,⊥

Institute for Cancer Research, Fox Chase Cancer Center, 7701 Burholme Avenue, Philadelphia, Pennsylvania 19111, Department of Chemistry and Department of Biochemistry and Biophysics, University of Pennsylvania, Philadelphia, Pennsylvania 19104, and Research and Development, Smith-Kline Beecham, King of Prussia, Pennsylvania 19406-0939

Received February 11, 1993; Revised Manuscript Received April 29, 1993

ABSTRACT: To provide a fluorescence probe for equilibrium and kinetic folding studies on ubiquitin, cassette mutagenesis in an *Escherichia coli* expression plasmid was used to replace the largely buried Phe 45 by a tryptophan. Under native conditions, the tryptophan fluorescence spectrum of this F45W mutant exhibits a blue-shifted emission maximum at 336 nm indicative of a largely solvent-shielded tryptophan environment. In contrast, the unfolded protein in 6 M guanidine hydrochloride (GuHCl) shows a 4-fold more intense emission band at 353 nm matching that of free tryptophan. The two-dimensional ^{1}H NMR spectrum of F45W ubiquitin was assigned by comparison with published assignments of the wild type. The mutation results in only limited chemical shift changes for residues in the immediate vicinity of residue 45. The structural similarity of F45W with wild-type ubiquitin was confirmed by a preliminary analysis of the nuclear Overhauser spectrum. NMR and circular dichroism measurements of the reversible GuHCl-induced unfolding transition show that the F45W mutation lowers the stability of the folded ubiquitin structure by less than 0.4 kcal/mol. The biological activity of the mutant was found to be indistinguishable from that of wild-type in terms of its reaction with the ubiquitin activating enzyme E_1 and an *in vitro* assay of ATP-dependent protein degradation. The kinetics of folding and unfolding of F45W ubiquitin was studied at two temperatures (8 and 25 °C) in a series of fluorescence-detected stopped-flow measurements over a wide range of GuHCl concentrations (0.5–6 M). The measurements at 25 °C are consistent with a two-state model with strongly denaturant-dependent folding and unfolding rates above about 2 M GuHCl. However, at lower denaturant concentrations, the rate of the major folding phase becomes GuHCl-independent, and up to 60% of the total fluorescence change occurs during the 2-ms dead time of the stopped-flow measurement. These observations provide clear evidence for the formation of an early folding intermediate during the first few milliseconds of refolding with a partially developed hydrophobic core involving Trp 45. The sigmoid denaturant dependence of the initial amplitude with an apparent midpoint of 1.3 M GuHCl suggests the presence of a discrete state that is destabilized at higher denaturant concentrations. In contrast, there is no evidence for an early intermediate in the folding kinetics at 8 °C. The destabilization of the intermediate at low temperature is consistent with a collapsed state stabilized primarily by hydrophobic interactions.

Recent efforts to elucidate the mechanism of protein folding have focused on structural and kinetic studies on small globular proteins (Kuwajima, 1989; Kim & Baldwin, 1990; Creighton, 1990; Matthews, 1991; Baldwin & Roder, 1991; Roder & Elöve, 1993). Much of the recent progress is due to advances in spectroscopic and kinetic techniques, especially NMR and hydrogen-exchange methods that make it possible to characterize transient folding intermediates in detailed structural terms (Udgaonkar & Baldwin, 1988; Roder et al., 1988). Another powerful approach makes use of site-directed mutagenesis to investigate the effect of specific amino acid changes on protein folding [e.g., Beasty et al. (1986), Wood et al. (1988), Goldenberg et al. (1989), and Matouschek et al. (1990, 1992)]. In spite of the diverse folding behavior observed for different proteins, some common features are beginning to emerge. For example, under mildly denaturing conditions, many proteins are found to undergo a transition from the native state to the so-called molten globule state, a compact nonnative state with a high content of secondary structure and partially disordered, fluctuating tertiary structure (Ptitsyn, 1987; Kuwajima, 1989; Baum et al., 1989; Hughson et al., 1990; Jeng et al., 1990). The observation of early kinetic intermediates with similar properties (Ikeguchi et al., 1986; Ptitsyn et al., 1990; Elöve et al., 1992) suggests that the collapse of the polypeptide chain into a compact intermediate may be a general phenomenon at early stages of protein folding.

In spite of its small size (76 residues), ubiquitin can fold into a very stable globular structure without relying on disulfide bonds, metal binding sites, or prosthetic groups for structural stabilization. As illustrated in Figure 1, the X-ray structure of ubiquitin (Vijay-Kumar et al., 1987) reveals a simple architecture rich in secondary structure, including a five-strand β-sheet with three antiparallel and one parallel pairs of strands, an α-helix (residues 23–34), a short 3_{10} helix (residues 56–59), and seven reverse turns. The curved β-sheet and the flanking α-helix enclose a single core of densely packed hydrophobic side chains, which is likely to contribute to the high stability of ubiquitin toward denaturation by heat, extremes of pH, and denaturing agents (Lenkinsiki et al., 1977; Briggs & Roder, 1992). However, because the denaturant and temperature dependence of the unfolding free energy is rather shallow, the stability under ambient conditions

† This work was supported by NIH Research Grant GM44881 (to H.R.), NIH Grant CA06927, and an appropriation from the Commonwealth of Pennsylvania to the Institute for Cancer Research.

* Address correspondence to this author at the Fox Chase Cancer Center.
‡ Fox Chase Cancer Center.
§ Department of Chemistry.
∥ Smith-Kline Beecham.
⊥ Department of Biochemistry and Biophysics.

0006-2960/93/0432-7054$04.00/0

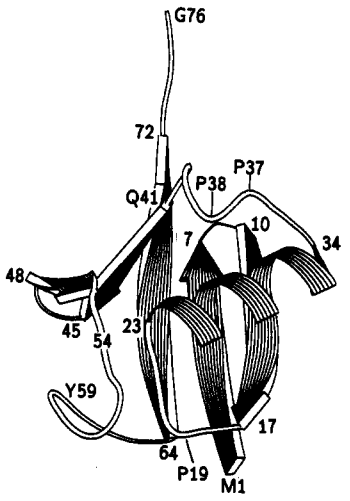

FIGURE 1: Ribbon diagram of wild-type ubiquitin based on the X-ray coordinates of Vijay-Kumar et al. (1987).

is not very high (~7 kcal/mol), which is typical for small proteins (Privalov, 1979; Alexander et al., 1992).

Briggs and Roder (1992) recently investigated the formation of hydrogen-bonded structure during ubiquitin folding by pulsed hydrogen exchange and 2D NMR techniques. Amide groups throughout the structure, including the α-helix, the β-sheet, and the helix–sheet interface, are protected against hydrogen exchange in a major cooperative folding phase with a time constant of about 8 ms. However, several amide protons are protected at a 2–3-fold slower rate, indicating that a peripheral loop near Tyr 59 (cf. Figure 1) and two hydrogen bonds connecting the two parallel strands of the β-sheet (Leu 67 and Leu 69) are formed in a subsequent step. The slow protection of two other probes (Gln 41 and Arg 42) during a final folding phase on the 10-s time scale can be attributed to nonnative cis peptide bonds preceding Pro 37 and Pro 38.

In terms of its structural and physical properties, ubiquitin is an excellent model for protein folding studies. However, it lacks suitable chromophores for conventional optical measurements of its stability and folding kinetics. The only potential optical probe is a single tyrosine residue, Tyr 59, which is exposed to the solvent and exhibits only small changes in fluorescence and absorbance upon folding (Jensen et al., 1980). To overcome this limitation, we introduced a fluorescence probe by replacing the largely buried Phe 45 with a tryptophan, making use of a cassette mutagenesis and bacterial expression system developed by Ecker et al. (1987a). In this study, we show that mutation of Phe 45 to Trp results in a biologically active ubiquitin variant with minimal changes in structure and stability. The presence of a sensitive fluorescence probe made it possible to study the kinetics of folding and unfolding under a wide range of conditions. The results provide evidence for the formation of a well-defined early folding intermediate with a partially assembled hydrophobic core during the first few milliseconds of refolding.

EXPERIMENTAL PROCEDURES

Materials. Bovine ubiquitin (Sigma Chemical Co.) was used without further purification. GuHCl[1] was of ultrapure grade from ICN-Schwarz/Mann. Deuterated GuHCl was prepared by three cycles of lyophilization from D_2O (99.9%, Isotech, Miamisburg, OH). GuHCl concentrations were based on refractive index measurements on a Reichert-Jung Mark II Abbe refractometer (Leica, Inc., New York). All other chemicals were of reagent grade. Restriction endonucleases and T_4 DNA ligase were purchased from New England Biolabs (Beverly, MA). Synthetic oligonucleotides were prepared at the DNA synthesis facility of the Fox Chase Cancer Center.

Preparation of F45W Ubiquitin. In previous studies of ubiquitin function, a synthetic gene coding for human ubiquitin, which corresponds to all known amino acid sequences for higher animal species (Wöstman et al., 1992), was prepared and expressed in *Escherichia coli* under the control of the heat-inducible λ P_L promoter (Ecker et al., 1987a). This pNMHUB plasmid has eight unique restriction sites in the ubiquitin coding region. For the Phe 45 to Trp mutation, the 34 base-pair cassette between the *Bsm*I and *Xho*I restriction sites was replaced with a synthetic DNA fragment containing the TGG codon for a Trp residue at position 45. Recombinant F45W clones were identified by the presence of a new *Sau*96I restriction site. The sequence of the mutated ubiquitin coding region was confirmed by double-stranded dideoxy sequencing. Ubiquitin expression in *E. coli* was induced by a temperature shift from 32 to 42 °C, as described previously (Ecker et al., 1987a). F45W was purified according to published procedures (Ciechanover et al., 1980; Ecker et al., 1987b), except for the final ion-exchange step, where we used a DEAE-Sephacel column. Pure ubiquitin fractions were eluted with 50 mM Tris, pH 8.3, at one void volume (150 mL). The fractions were analyzed by SDS–PAGE (15% gels). Protein concentrations for F45W were based on an extinction coefficient of 6744 M^{-1} cm^{-1} at 280 nm estimated according to the method of Gill and von Hippel (1989).

NMR Spectroscopy. All NMR experiments were performed at 600.13 MHz on a Bruker AM 600 spectrometer. Two-dimensional ^1H NMR spectra were recorded at 30 °C on 4 mM solutions of WT and F45W ubiquitin in 90% H_2O/10% D_2O containing 25 mM deuterated sodium acetate and 25 mM sodium phosphate at pH 5.8, the conditions used by Di Stefano and Wand (1987) in the proton resonance assignment of WT ubiquitin. Phase-sensitive NOESY (Macura & Ernst, 1980; Anil-Kumar et al., 1980), DQF-COSY (Shaka & Freeman, 1983; Rance et al., 1984), and TOCSY (Braunschweiler & Ernst, 1983; Bax & Davis, 1985) spectra were recorded with time proportional phase incrementation (Marion & Wüthrich, 1983). For all experiments, a spectral width of 7352.9 Hz was used in both dimensions and the water resonance was suppressed by selective saturation during a 2.5-s delay preceding the first pulse, as well as during the mixing period of the NOESY experiment. For NOESY and DQF-COSY spectra, 64 scans of 2048 complex data points were averaged for 750 increments ranging from 34 μs to 51 ms. The mixing time for NOESY experiments was 150 ms. TOCSY spectra were recorded with a 65-ms MLEV-17 mixing sequence (Bax & Davis, 1985), collecting 16 scans of 1024 complex points for 512 increments (34 μs–35 ms). The data were processed and analyzed on a Silicon Graphics Iris workstation with the program Felix (Hare Research, Woodinville, WA). The filter functions used were 60° shifted sine windows for NOESY and TOCSY spectra and unshifted sine windows for DQF-COSY spectra in both dimensions. The final data matrix was 2048 × 2048 real points (3.6 Hz/point resolution) for NOESY and DQF-COSY spectra and 1024 × 1024 points (7.2 Hz/point) for TOCSY spectra.

[1] Abbreviations: GuHCl, guanidine hydrochloride; WT, wild-type ubiquitin; F45W, ubiquitin variant with Trp substituted for Phe 45; NOESY, nuclear Overhauser spectroscopy; DQF-COSY, double-quantum filtered correlated spectroscopy; TOCSY, total correlation spectroscopy; NOE, nuclear Overhauser effect; CD, circular dichroism; SDS–PAGE, SDS–polyacrylamide gel electrophoresis.

Equilibrium Unfolding Measurements. For GuHCl titrations, stock solutions of native protein in buffer and unfolded protein in about 7 M GuHCl were prepared at the same protein concentration in 25 mM acetate at pH 5.0 or 20 mM phosphate at pH 2.5. After the pH was adjusted, each solution was filtered through a 0.2-μm membrane and equilibrated for at least 1 h at 25 °C. Appropriate ratios of the native and unfolded solutions were mixed to prepare samples at intermediate GuHCl concentrations for equilibrium unfolding experiments. These were individually equilibrated for at least 15 min before measurements. The final GuHCl concentration of each sample was determined by refractometry.

For one-dimensional NMR studies of GuHCl denaturation, protein concentrations of about 1 mM were used to prevent aggregation (line broadening indicative of dimer formation was observed for WT ubiquitin above 3 mM but not for F45W, which appears to be more soluble). For complete exchange of the amide protons, an unbuffered solution of the native protein was titrated to pD 9.5 (uncorrected pH meter reading) and incubated at 45 °C for 90 min prior to the preparation of NMR samples. NMR spectra were recorded at 25 °C for a series of samples in D_2O buffer (25 mM deuterated sodium acetate, pD 5) at increasing concentrations of GuHCl. At each GuHCl concentration, the NMR probe was tuned and matched. The length of a 90° pulse was found to increase with increasing ionic strength. For each spectrum, 512 transients of 32K complex data points covering a spectral width of 8065 Hz were acquired at a total recycling time of 4.5 s. The spectra were processed and integrated on the Aspect 3000 computer of the spectrometer.

CD experiments were performed on an Aviv 62DS CD spectrometer. The observation cell was thermostated at 25 °C by means of a Peltier device. Protein concentrations were approximately 60 μM for measurements in a 1-mm cuvette. For GuHCl denaturation curves, the ellipticity at 222 nm was recorded in the kinetic mode, taking an average of 60 points recorded in a 1-min trace. The ellipticity at 250 nm was recorded for each sample and used as a baseline value.

Fluorescence measurements were performed on an AMINCO-Bowman Series 2 luminescence spectrometer (SLM-AMINCO, Urbana, IL). Sample temperature was controlled to within ±0.2 °C with a water-jacketed cuvette holder and a circulating water bath. The concentration of F45W ubiquitin was ~30 μM for fluorescence measurements in a square 1-cm quartz cuvette. The excitation wavelenth was 285 nm (2-nm bandpass), and the emission was observed at 353 nm (4-nm bandpass). The fluorescence signal was corrected for lamp fluctuations by taking the ratio of the emission signal to a reference signal measured by a photodiode. Each measurement was an average of 30 data points collected in a 1-min time trace.

Stopped-Flow Fluorescence Measurements. Fluorescence-detected folding and unfolding experiments were performed on a PQ/SF-53 stopped-flow instrument (Hi-Tech, Salisbury, England) equipped with a Berger-type mixing chamber and a 2 × 2 × 10 mm flow cell. The dead time of the instrument is estimated to be about 2 ms. The stopped-flow module and observation cell were thermostated by circulating water from a temperature-controlled water bath. A 75-W xenon lamp (On-Line Instrument Systems, Inc., Jefferson, GA) and a monochromator (Hi-Tech) were used for excitation at 285 nm (5-nm bandwidth) along the 10-mm axis of the flow cell. The fluorescence emission was measured in the 2-mm direction, using a high-pass glass filter with a 320-nm cutoff (filter WG-320 provided by Hi-Tech). For refolding experiments, a solution of unfolded F45W in 6 M GuHCl (25 mM acetate, pH 5.0) was diluted 6-fold with refolding buffer at pH 5.0 containing different amounts of GuHCl to yield final concentrations ranging from 1 to 6 M and a final protein concentration of 30 μM. For measurements at lower GuHCl concentrations (0.5–1 M), an 11-fold dilution and correspondingly higher initial protein concentrations were used. For unfolding experiments, a solution of native F45W in 2 M GuHCl was unfolded by 6-fold dilution with concentrated GuHCl buffer solution to yield final concentrations between 3.5 and 6 M GuHCl. The fluorescence changes associated with refolding or unfolding were recorded at a sampling time of 64 μs using a personal computer equipped with a DT-2801/A data acquisition board (Data Translation, Inc., Marlboro, MA) and a program written in ASYST language (Asyst Software Technologies, Inc., Rochester, NY) that uses logarithmic averaging to record a complete kinetic trace (from 64 μs to ~100 s) in a single experiment. Typically, three traces were averaged at each GuHCl concentration. Kinetic parameters were obtained by nonlinear least-squares fitting of two or three exponential phases, using a program based on the ASYST software package.

Ubiquitin Activity. An ATP–pyrophosphate exchange assay described by Haas and Rose (1982) was used to measure the interaction of WT and F45W ubiquitin with the ubiquitin activating enzyme E_1. F45W was incubated at 37 °C with E_1 and [^{32}P]pyrophosphate in 50 mM Tris-HCl, pH 7.6, 10 mM $MgCl_2$, and 0.1 mM dithiothreitol, and the exchange of radioactivity into ATP was monitored. Ubiquitin-dependent proteolysis was assayed according to the method of Hershko et al. (1983). Pure WT and F45W ubiquitin were separately incubated with fraction II obtained from reticulocytes (Ciechanover et al., 1978), using ^{125}I-labeled reduced carboxymethylated bovine serum albumin as the substrate.

RESULTS

Design and Preparation of a Trp-Containing Ubiquitin. In selecting a site for mutation to Trp we focused on the two phenylalanines of ubiquitin, Phe 4 and Phe 45. Tyr 59 was not considered because the hydrogen bond between its side-chain hydroxyl and the backbone amide of Glu 51 appears to be structurally important. Inspection of the crystal structure of ubiquitin (Vijay-Kumar et al., 1987), using the molecular graphics program Quanta (Molecular Simulations Inc., Waltham, MA), showed that the Phe 4 side chain is in a peripheral location on the outer surface of the β-sheet with 26% of its surface area exposed to the solvent. Phe 45, on the other hand, is sandwiched between the β-sheet and α-helix at the edge of the hydrophobic core (cf. Figure 1). A fluorophore at position 45 will report on changes occurring within the ubiquitin core and thus would be a suitable probe for global folding events. Because the side chain of Phe 45 is about 97% buried, replacement of Phe 45 by Trp is likely to lead to a large fluorescence change upon refolding due to burial of the tryptophan ring in the apolar interior of the protein. Furthermore, residue 45 is close enough to the protein surface to accommodate the bulky tryptophan ring without risking major structural perturbations.

Phe 45 was mutated to Trp by cassette mutagenesis, and the F45W protein was produced by using a previously developed (Ecker et al., 1987a) *E. coli* expression system (see Experimental Procedures). Each liter of culture yielded about 15 mg of F45W ubiquitin that was judged pure by SDS–PAGE (15% gel). This yield is comparable to that of recombinant WT ubiquitin in the same expression system.

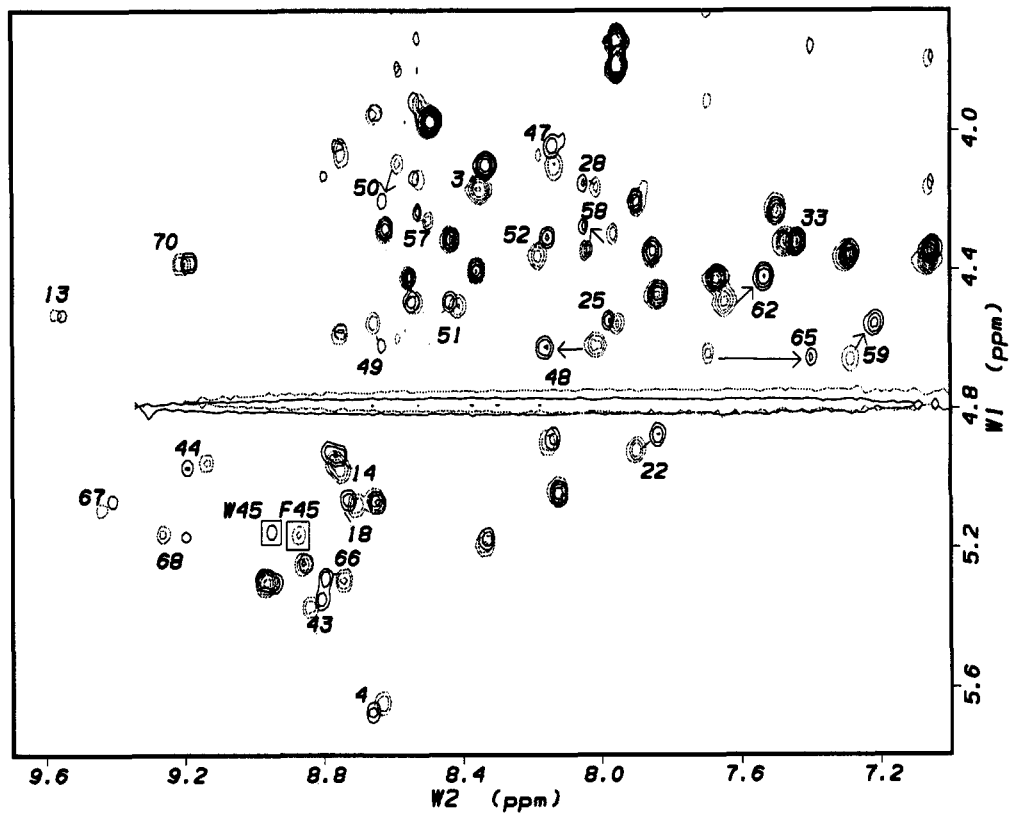

FIGURE 2: Comparison of TOCSY fingerprint regions for WT and F45W ubiquitin. Combined plots of NH–C_αH cross peaks for WT (dashed contours) and F45W (solid contours) are shown. The boxed cross peaks correspond to the site of mutation. Residues with significant chemical shift differences (≥0.04 ppm) are labeled. Arrows connect corresponding cross peaks from WT to F45W.

Characterization of F45W by Two-Dimensional NMR. For the assignment of the ^{1}H NMR spectrum of F45W ubiquitin, we were able to take advantage of a nearly complete set of resonance assignments for WT ubiquitin reported by Di Stefano and Wand (1987) and Weber et al. (1987). TOCSY, DQF-COSY, and NOESY spectra of WT and F45W ubiquitin were recorded under conditions matching those used by Di Stefano and Wand (90% H_2O/10% D_2O, 25 mM phosphate, 25 mM acetate, pH 5.8, and 30 °C). Comparison of the NH–C_αH cross peak region in the TOCSY spectra of WT and F45W in Figure 2 shows that the mutation results in only minor chemical shift changes for the majority of the main-chain protons. Thus, it was possible to assign about 70% of the NH–C_αH cross peaks (including Trp 45) in the TOCSY and DQF-COSY spectra by direct comparison with the corresponding WT spectra. The assignments were confirmed and further extended by using the TOCSY spectra to identify characteristic cross peak patterns between amide and side-chain protons. Even in cases where the main-chain resonances experience large shift changes, these long-range connectivities can be easily recognized. Finally, most assignments were checked by tracing the sequential connectivities in the NOESY spectrum of F45W. The NOE patterns observed in the α-helix and the β-sheet were in full agreement with those reported for the WT (Di Stefano & Wand, 1987; Weber et al., 1987), confirming that the secondary structure of ubiquitin remains unperturbed by the F45W mutation.

The main-chain protons of 25 residues undergo chemical shift changes of at least 0.04 ppm upon mutation (cf. labeled cross peaks in Figure 2). The NH and/or C_αH resonances of six residues exhibit chemical shift changes (F45W–WT) over 0.1 ppm, including Ala 46 NH (–0.38 ppm) and C_αH (–0.2), Lys 48 NH (0.16 ppm), Leu 50 C_αH (0.12 ppm), Leu 61 C_αH (–0.2 ppm), Gln 62 NH (–0.12 ppm), and Ser 65 NH (–0.3 ppm). However, the largest shifts are found for some of the aliphatic core residues. For example, one of the C_γ methylene protons of Ile 61 moves from –0.37 ppm in WT to –0.9 ppm in F45W. In the WT structure, the Ile 61 side chain lies directly above the Phe 45 ring, and the 0.53 ppm upfield shift in the mutant can be explained in terms of the change in ring current effect associated with the Phe to Trp mutation.

In a preliminary analysis of the NOESY data, we have focused on NOEs between the Trp 45 ring and surrounding core residues in the mutant protein. An expanded region of the NOESY spectrum of F45W is plotted in Figure 3, which shows a number of well-resolved NOE cross peaks between Trp 45 ring protons and several hydrophobic residues, including Ala 46, Leu 50, Tyr 59, Ile 61, and Leu 67. All of these residues are in close proximity with Phe 45 in the WT ubiquitin structure and exhibit a similar set of NOEs. These observations, together with the chemical shift changes mentioned above, show that the tryptophan occupies the same pocket and has a similar ring-plane orientation as the Phe 45 side chain that it replaces. Furthermore, a qualitative analysis of the NOE patterns allowed us to distinguish between two opposite orientations of the tryptophan ring. The five-membered ring of Trp 45 appears to be most deeply buried with the indole NH and one edge of the six-membered ring facing the surface.

Effect of F45W Mutation on Stability. The stability of F45W was compared to that of WT ubiquitin by using several spectroscopic probes to monitor the GuHCl-induced unfolding transition at equilibrium. The conditions chosen for most experiments (pH 5.0, 25 °C) match those of previous kinetic folding studies by pulsed hydrogen exchange (Briggs & Roder, 1992).

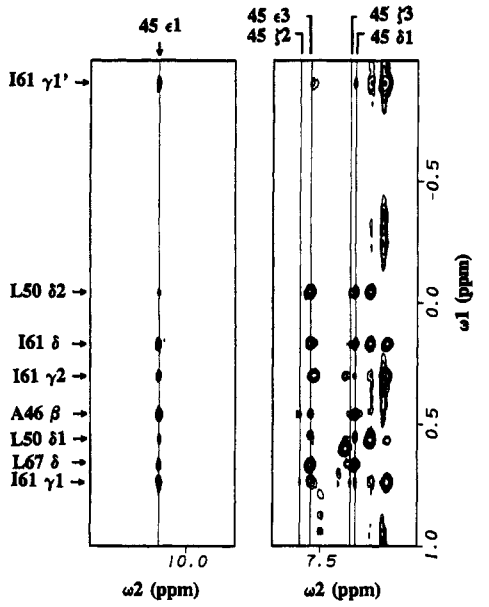

FIGURE 3: Expanded plots of the NOESY spectrum of F45W containing cross peaks between aromatic and aliphatic protons. Cross peaks to the ring protons of Trp 45 are labeled.

^{1}H NMR is a convenient method to observe the equilibrium between folded and unfolded states (Wüthrich et al., 1980; Roder, 1989; Briggs & Roder, 1992). The aromatic region of the proton NMR spectrum for WT and F45W ubiquitin in D_2O is shown in Figure 4 at several GuHCl concentrations. The observation of distinct resonances for the folded and unfolded molecules shows that the two states undergo slow interconversion on the NMR time scale. There is no evidence for any intermediate states since folded and unfolded resonances are the only ones observed. Furthermore, unfolding of WT and F45W ubiquitin is fully reversible, on the basis of the observation that spectra recorded after dilution of the denaturant from 6 M to 0.5 M GuHCl are indistinguishable from those of freshly prepared samples that were never unfolded. Well-resolved resonances for both folded and unfolded forms are found for the His 68 C_2 ring proton near 8 ppm and the Tyr 59 C_ϵ protons near 7 ppm. From the integrated resonance intensities in the folded (I_f) and unfolded (I_u) states, the fraction of unfolded molecules, $f_u = I_u/(I_f + I_u)$, was determined at several GuHCl concentrations throughout the transition. The transition curves were calculated by nonlinear least-squares analysis, based on a two-state model with linear dependence of the free energy of unfolding, ΔG, on the denaturant concentration, C (Tanford, 1970; Pace, 1986)

$$\Delta G = \Delta G(0) - mC = m(C_m - C) \qquad (1)$$

where $\Delta G(0)$ is the free energy in the absence of denaturant, and C_m is the denaturant concentration at the midpoint of the transition where $\Delta G = 0$. The transition curves observed for Tyr 59 and His 68 ring protons are within experimental error, confirming the two-state nature of the ubiquitin folding–unfolding equilibrium. The parameters describing the transition curves for WT and F45W ubiquitin are listed in Table I. The free energy difference measured in the transition region (at 3.8 M GuHCl) shows that the folded state is destabilized by ~0.4 kcal/mol due to the mutation.

Under native conditions, the far-UV CD spectra of F45W and WT are very similar. Both exhibit a prominent negative band at 208 nm that can be attributed to the β-sheet and a smaller band at 222 nm due to the α-helix. Small differences

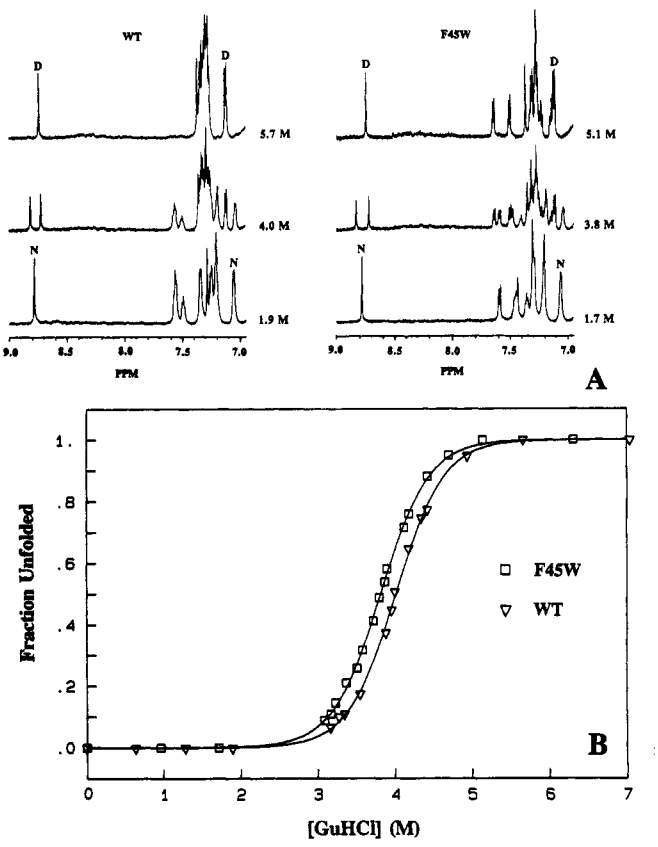

FIGURE 4: GuHCl-induced unfolding of WT and F45W monitored by one-dimensional ^{1}H NMR. Panel A shows the aromatic region for WT and F45W at the indicated concentrations of denaturant at 25 °C and pD 5.0. Resonances of His 68 C_2 proton (downfield) and Tyr 59 C_ϵ protons (upfield) in the native (N) and denatured (D) states are labeled. Panel B shows equilibrium unfolding transition curves for WT (▽) and F45W (□) generated by integration of the native and unfolded His 68 C_2H peaks. Solid lines are nonlinear least-squares fits based on a two-state model with linear dependence of unfolding free energy on denaturant concentration (eq 1).

observed between 205 and 225 nm are probably due to the contribution of Trp 45 to the far-UV CD spectrum. In 6 M GuHCl, both forms of ubiquitin show a strongly reduced negative ellipticity at 222 nm. The change in ellipticity at 222 nm was used to monitor the unfolding transition for both forms of ubiquitin, and the corresponding equilibrium parameters are reported in Table I. As in the NMR measurements, the transitions for WT and F45W ubiquitin are very similar, indicating a slightly lower stability for the mutant form (0.3 kcal/mol). The close agreement between the CD and NMR data provides further support for the validity of the two-state analysis.

Fluorescence of F45W Ubiquitin. The tryptophan fluorescence spectrum of F45W under native conditions (pH 5.0 or 2.4, at 25 °C) shows a blue-shifted emission maximum at 336 nm as expected for a tryptophan in a partially solvent-shielded environment (Stryer, 1968). Upon unfolding in 6 M GuHCl, the emission maximum shifts to 353 nm and increases in intensity by a factor 4. Comparison with an equimolar sample of *N*-actyl-L-tryptophanamide under the same solvent conditions shows that the fluorescence spectrum of unfolded F45W is very similar to that of free tryptophan (Figure 5, inset). Thus, Trp 45 appears to be fully exposed to the solvent at 6 M GuHCl.

The increase in fluorescence intensity at 353 nm was used to monitor the unfolding equilibrium of F45W. The fluorescence results at pH 5 are in excellent agreement with the

Table I: Effect of F45W Mutation on Stability Measured by GuHCl Denaturation[a]

		wild-type			F45W			
method	condition	C_m (M)	m (kcal mol^{-1} M^{-1})	$\Delta G(0)$ (kcal mol^{-1})	C_m (M)	m (kcal mol^{-1} M^{-1})	$\Delta G(0)$ (kcal mol^{-1})	$\Delta\Delta G$(C)[b] (kcal mol^{-1})
NMR	pD 5	4.01	1.88	7.5	3.82	1.87	7.1	0.37
far-UV CD	pH 5	3.85	1.75	6.7	3.69	1.98	7.3	0.32
fluorescence	pH 5				3.65	1.92	7.0	
fluorescence	pH 2.4				3.52	1.79	6.3	
NMR[c]	pD 3.5	3.7	1.35	5.0				

[a] All measurements were performed at 25 °C. The midpoint concentration C_m and the slope m were determined by nonlinear least-squares analysis of the GuHCl unfolding curves. The free energy in the absence of GuHCl, $\Delta G(0)$, was calculated according to eq 1. Typical experimental errors estimated by systematic variation of the fit parameters (including baselines) are ±2% for C_m and ±5% in m. The uncertainty in the $\Delta G(0)$ is larger (10–20%) due to error propagation. [b] Free energy change ΔG(WT) − ΔG(F45W) at 3.8 M GuHCl. [c] From Briggs and Roder (1992).

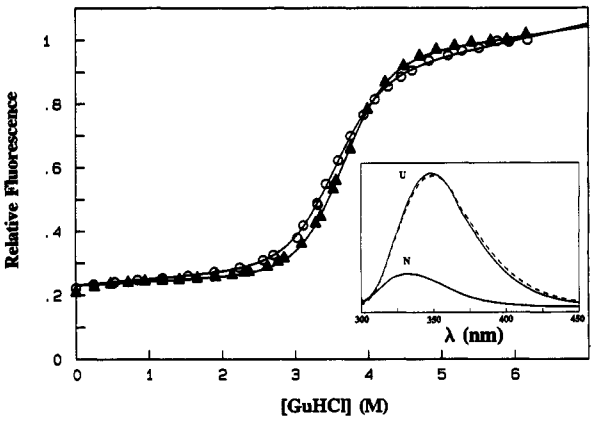

FIGURE 5: Fluorescence-detected GuHCl denaturation of F45W. Equilibrium unfolding transition curves were monitored by the fluorescence at 353 nm at pH 5.0 (▲) and 2.4 (○), both at 25 °C. Solid lines are nonlinear least-squares fits as in Figure 4. The inset shows the relative fluorescence of native (N) and unfolded (U) F45W; the dashed line corresponds to the fluorescence spectrum of an equimolar solution of *N*-acetyl-L-tryptophanamide in 6 M GuHCl.

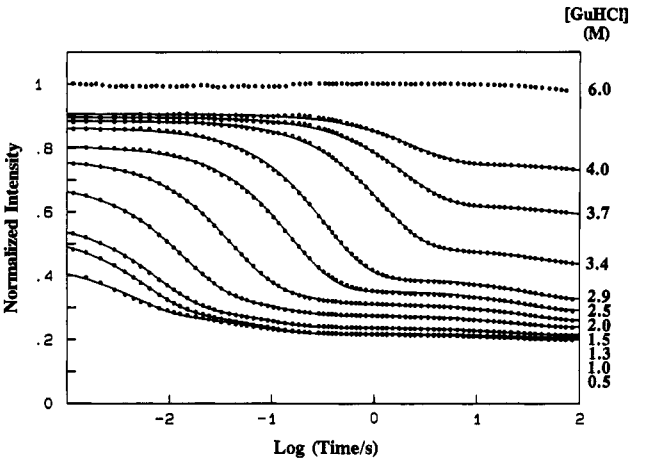

FIGURE 6: Fluorescence-detected stopped-flow kinetic traces of F45W refolding at 25 °C (pH 5), plotted on a logarithmic time scale. Traces obtained at the indicated final GuHCl concentrations were normalized to the signal intensity for unfolded protein in 6 M GuHCl (top trace). The solid lines represent best fits of two (≥3.4 M GuHCl) or three (≤2.9 M GuHCl) exponential phases calculated by nonlinear least-squares analysis (see Figure 7 for the rates and amplitudes of the major phase).

NMR and CD data (Table I). At pH 2.4, the midpoint of the GuHCl-induced transition is only slightly lower than that at pH 5, but the slope, m, is about 10% smaller (Figure 5). A decrease in m value toward acidic pH was also observed in previous NMR equilibrium unfolding results on the WT at pD 3.5 (Briggs & Roder, 1992; cf. Table I).

Fluorescence-Detected Kinetics of the Folding–Unfolding Reaction of F45W. We used systematic stopped-flow measurements as a function of GuHCl concentration for a detailed kinetic characterization of folding and unfolding of F45W at 25 and 8 °C. The folding kinetics at 25 °C following a rapid jump from 6 M to various final GuHCl concentrations is shown in Figure 6. Below about 2 M GuHCl, the fluorescence changes are characterized by four distinct kinetic phases. At 1 M GuHCl, for example, about 50% of the total fluorescence change occurs during the 2-ms dead time of the stopped-flow measurement [following Kuwajima et al. (1991), we refer to this initial change as the "burst phase"]. The remaining decrease in fluorescence occurs in a fast phase (73% of the observable amplitude) with a time constant τ = 5 ms, an intermediate phase with τ = 75 ms (22% amplitude), and a minor slow phase with $\tau \sim 20$ s (~5% amplitude). Above 2.5 M GuHCl, the kinetic changes are characterized by a major exponential phase that accounts for about 90% of the amplitude and a minor slow phase. A single-exponential phase was observed in stopped-flow unfolding experiments (not shown), starting with folded F45W in 2 M GuHCl and jumping to final GuHCl concentrations above 3.5 M. In Figure 7A, the logarithm of the rate for the major phase of folding or unfolding at 25 °C is plotted as a function of GuHCl concentration. The V-shaped log(k) vs [GuHCl] plot goes through a minimum at about 4 M GuHCl, near the midpoint of the corresponding equilibrium transition (3.65 M). The rate of the intermediate phase also decreases with increasing GuHCl concentration (not shown), but the slope is smaller than that of the major phase, so that the two processes merge below the unfolding transition where their rates coincide. Under all conditions, a minor slow folding phase is observed with an essentially GuHCl-independent time constant of about 20 s. According to the pulsed hydrogen-exchange results of Briggs and Roder (1992), this slow phase can be attributed to a minor population of slowly folding molecules for which cis–trans isomerization of the Pro 19 peptide bond is the rate-limiting step. However, the origin of the intermediate phase is less apparent, since its rate (130 s^{-1} at 25 °C) appears to be too fast for proline isomerization.

In analogy to eq 1, the denaturant dependence of the observed rate, k_{obs}, for a two-state folding–unfolding reaction can be modeled as follows [Tanford, 1970; cf. Jackson and Fersht (1991)]

$$k_{obs} = k_f + k_u \quad (2)$$

with

$$\ln k_f = \ln k_f(0) - m_f C/RT$$

$$\ln k_u = \ln k_u(0) + m_u C/RT$$

where $k_f(0)$ and $k_u(0)$ are the folding and unfolding rates in the absence of denaturant and m_f and m_u are the corresponding

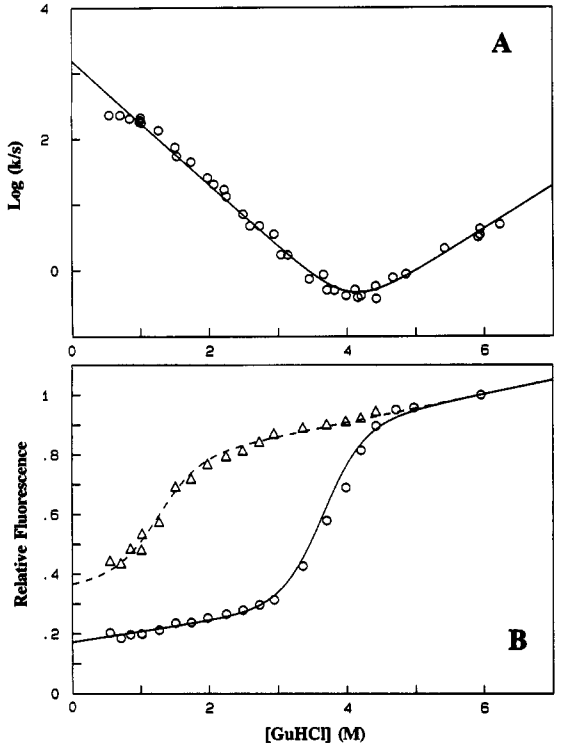

FIGURE 7: Analysis of folding and unfolding kinetics of F45W at 25 °C and pH 5.0. Panel A shows a V-shaped log (k) vs [GuHCl] plot, where k is the rate of the single unfolding ([GuHCl] > 4 M) and major observable refolding ([GuHCl] < 4 M) phases. The solid line represents a fit of a two-state model according to eq 2 with $k_f(0)$ = 1532 s^{-1}, $k_u(0) = 4.3 \times 10^{-4}$ s^{-1}, m_f = 1.3 kcal mol^{-1} M^{-1}, and m_u = 0.9 kcal mol^{-1} M^{-1}. Panel B shows the final fluorescence intensities at long times (○) and initial intensities obtained by extrapolating the fitted stopped-flow refolding traces (shown in Figure 6) to zero time (△) (both normalized to the signal of F45W in 6 M GuHCl) as a function of GuHCl concentration. The solid curve is the equilibrium unfolding transition of F45W monitored by fluorescence at 25 °C and pH 5.0 shown in Figure 5. The minor discrepancy between the data points and the curve is probably due to the difference in sample conditions. The dashed curve represents a two-state transition (cf. Figure 4) for the burst-phase intermediate with C_m = 1.3 M and m = 1.9 kcal mol^{-1} M^{-1}.

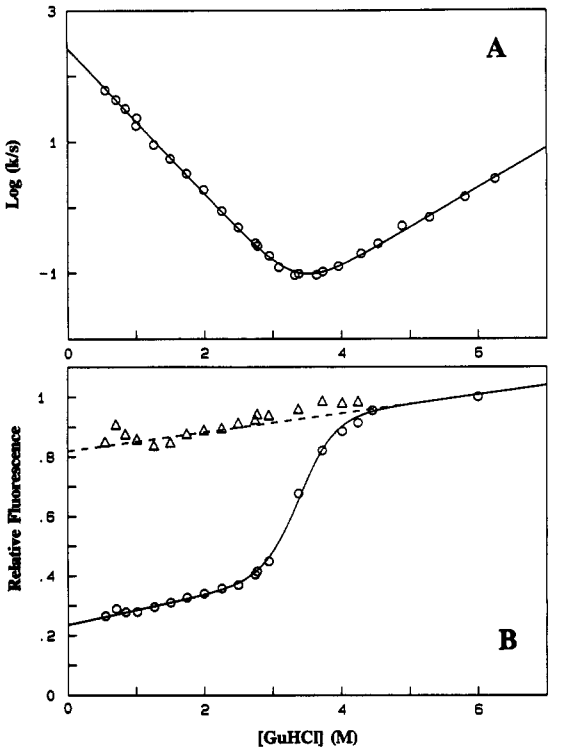

FIGURE 8: Analysis of folding and unfolding kinetics for F45W observed by stopped-flow fluorescence measurements at 8 °C and pH 5.0. As in Figure 7, panel A shows a log (k) vs [GuHCl] plot for the major folding and single unfolding phases. Parameters obtained for the solid line (cf. Figure 7) are k_f = 264 s^{-1}, $k_u = 4.7 \times 10^{-4}$ s^{-1}, m_f = 1.4 kcal mol^{-1} M^{-1}, and m_u = 0.8 kcal mol^{-1} M^{-1}. Panel B shows the initial (△) and final (○) fluorescence amplitudes plotted as a function of GuHCl concentration. The solid curve represents a two-state transition (cf. Figure 4) with C_m = 3.5 M and m = 2.1 kcal mol^{-1} M^{-1}. The dashed line is the estimated fluorescence signal of the unfolded state by linear extrapolation from the denatured baseline region.

slopes. The solid curve in Figure 7A shows that the denaturant dependence of the observed rates above 1 M GuHCl is fully consistent with eq 2. The corresponding fit parameters are given in the legend.

The initial fluorescence amplitudes, obtained by extrapolation of the kinetic traces to t = 0, and the final values of the kinetic traces at long times (~100 s) are plotted in Figure 7B as a function of GuHCl concentration. In the refolding experiments at 25 °C, the initial amplitude deviates markedly from the fluorescence expected for the fully unfolded form at GuHCl concentrations below 2 M. This is a clear indication of an unresolved rapid folding event that leads to the formation of a burst-phase intermediate. The GuHCl dependence of the initial amplitude can be fit by a sigmoid transition curve with a midpoint of about 1.3 M GuHCl and an m value similar to that of the equilibrium transition. Furthermore, below 1 M GuHCl, the linear dependence of log(k) on GuHCl concentrations is sharply interrupted and the rate levels off at a value of about 200 s^{-1} (Figure 7A). These observations provide strong evidence for the formation of an early folding intermediate with a partially buried tryptophan during the first few milliseconds of refolding.

In a similar series of stopped-flow experiments on F45W at 8 °C, but otherwise identical conditions, we also observed one major and two minor folding phases at low denaturant concentrations. For example, at 1 M GuHCl, 75% of the overall fluorescence change occurs in a 57-ms phase, followed by a 18% decrease in an intermediate phase with τ = 0.5 s and a final process (7%) with a ~100-s time constant. Above 2 M GuHCl, the kinetics is again biphasic with a major fast and a minor slow phase. However, in contrast to the measurements at 25 °C, we found no evidence for a burst-phase intermediate (Figure 8). For the major folding phase, log(k) increases linearly with decreasing GuHCl concentration down to the lowest value measured (0.5 M), and the initial amplitude corresponds to the fluorescence of the unfolded protein under refolding conditions (dashed line in Figure 8B), as expected for a two-state folding reaction.

Biological Activity of F45W Ubiquitin. F45W was tested in two different assays to determine its ability to participate in the ubiquitin and ATP-dependent proteolysis system. First, the ATP–PP_i exchange reaction was used to monitor the ability of the ubiquitin activating enzyme (E_1) to catalyze the ubiquitin-dependent exchange of radioactivity between pyrophosphate and ATP (Haas & Rose, 1982). E_1 catalyzes the adenylation of ubiquitin at the carboxy terminal glycine residue (Gly 76). We found that, within experimental error, F45W is as active as WT (K_m = 0.83 and V_{max} = 50 s^{-1} for F45W, compared to K_m = 0.77 and V_{max} = 42 s^{-1} for WT). Second, F45W was tested for its ability to mediate ATP-dependent proteolysis *in vitro*, using radiolabeled bovine serum albumin (reduced and carboxymethylated) as an exogenous substrate (Hershko et al., 1983). The F45W variant was also

indistinguishable from WT ubiquitin with respect to this more global assay of ubiquitin function.

DISCUSSION

We have incorporated a sensitive fluorescence probe into ubiquitin by using site-directed mutagenesis to replace a phenylalanine at position 45 with a tryptophan. A preliminary structural analysis by two-dimensional ^{1}H NMR methods shows that the solution structure of the F45W mutant is very similar to that of WT ubiquitin, except for small structural rearrangements near the site of mutation. Only a few residues in the immediate vicinity of residue 45 undergo significant chemical shift changes. Some of the largest spectral changes are observed for amide protons, which are especially sensitive to changes in hydrogen-bonded structure, and other differences can be attributed to changes in ring current effects associated with the Phe to Trp mutation. Qualitative analysis of NOEs between protons of the Trp 45 ring and surrounding residues indicates that the tryptophan side chain lies approximately in the same plane as the Phe 45 ring in the WT ubiquitin structure with only one edge of the six-membered ring exposed to the solvent. We are now using restrained molecular dynamics and relaxation matrix methods to refine the structure of F45W, based on a more complete set of NMR distance constraints.

Upon folding, the fluorescence emission maximum of F45W ubiquitin shifts from 353 to 336 nm and decreases by a factor 4 in intensity (Figure 5). The blue shift is consistent with a tryptophan environment partially shielded from solvent (Stryer, 1968), and the decrease in intensity appears to be due to intramolecular fluorescence quenching, although the origin of this quenching reaction is unclear. In any case, the large fluorescence change associated with the folding transition provides a sensitive empirical probe for equilibrium and kinetic folding studies.

To measure the effect of the Phe 45 to Trp replacement on the stability of the ubiquitin structure, we used ^{1}H NMR and far-UV CD to monitor the GuHCl-induced unfolding transition for both forms of the protein under identical conditions (pH 5, 25 °C). Analysis of the equilibrium measurements in terms of a two-state model shows that in the transition region the folded state of F45W is about 0.4 kcal/mol less stable than WT (Table I). The small magnitude of this destabilization, compared to a total unfolding free energy of about 7 kcal/mol in the absence of denaturant, confirms that the mutation results in only minor structural perturbations. The fluorescence-detected unfolding transition for F45W is in excellent agreement with the CD and NMR data, which confirms the validity of the two-state analysis. At pH 2.4, the midpoint of the unfolding transition, C_m, and its slope, m, are slightly lower than at pH 5, which is consistent with previous NMR results on WT ubiquitin at pD 3.5 (Briggs & Roder, 1992). The small decrease in C_m shows that ubiquitin is unusually stable at acidic pH. The m value at low pH is also unusual, since several other proteins show a significant increase in m values when the pH is lowered. For example, Pace et al. (1992) observed a 60% increase between pH 7 and 3 in the m value for barnase, which they attributed to an increased solvent exposure of the denatured state at low pH. The opposite trend observed for ubiquitin can be explained by an increase in (hydrophobic) surface area in the folded conformation at low pH. This effect may be related to the observation that the tyrosine fluorescence of ubiquitin increases at acid pH due to the loss of a hydrogen bond between the Tyr 59 OH and the backbone NH of Glu 51 (Jensen et al., 1980), promoting further exposure of the tyrosine side chain to the solvent.

The presence of a tryptophan in F45W ubiquitin enables us to make use of fluorescence-detected stopped-flow experiments for a systematic analysis of the kinetics of folding and unfolding under a wide range of conditions. Relaxation studies as a function of denaturant concentration provide valuable information on folding intermediates and the nature of the rate-determining steps involved and are thus the method of choice for a comprehensive kinetic characterization of protein folding [e.g., Tanford (1968), Matthews (1987), Kuwajima et al. (1989) and Matouschek et al. (199)]. At both temperatures studied, the kinetic behavior above 2 M GuHCl is indicative of a cooperative folding/unfolding reaction without significant population of intermediates. Except for a minor slow phase caused by a small population of molecules with nonnative proline isomers, the kinetics of F45W exhibits a single-exponential phase with a strongly GuHCl-dependent rate. The V-shaped dependence of $\log(k)$ on GuHCl concentrations for the dominant phase (Figures 7A and Figure 8A) with a linear decrease below C_m and a linear increase above is characteristic for a two-state reaction (cf. eq 2). Furthermore, the equilibrium transition can be approximated quite well by the GuHCl-dependent folding and unfolding rates, k_f and k_u. For a two-state reaction with an equilibrium constant $K_{eq} = k_u/k_f$, eq 2 predicts that the sum of the slopes from the kinetic data, $m_{pred} = m_f + m_u$, corresponds to the slope of the equilibrium transition (eq 1). The close agreement between m_{pred} (2.2 kcal mol^{-1} M^{-1} at both temperatures; cf. Figures 7 and 8) and the observed equilibrium m values (1.9 kcal mol^{-1} M^{-1} at 25 °C and 2.1 kcal mol^{-1} M^{-1} at 8 °C) represents a stringent test for the two-state model. Moreover, the minimum of the V-plot for the kinetic data at 8 °C agrees well with the midpoint of the equilibrium unfolding transition (Figure 8). However, at 25 °C the minimum of the $\log(k)$ plot (4 M) is noticeably higher than the C_m for the equilibrium transition (3.65 M). At this time, it is unclear whether this discrepancy reflects a genuine deviation from ideal two-state behavior or whether it is due to experimental factors (cf. legend to Figure 7).

On the other hand, the folding kinetics at 25 °C below 2 M GuHCl is inconsistent with a simple two-state model. First, the deviation from linearity in the $\log(k)$ plot below 1 M GuHCl (Figure 7A) indicates that under these conditions the formation of an intermediate state becomes rate-limiting, as previously observed for a number of proteins [e.g., Matouschek et al. (1990)]. A second more striking demonstration for the formation of an early intermediate is provided by the sharp decrease in the initial fluorescence signal observed below 2 M GuHCl (Figure 7B). At 0.5 M GuHCl, for example, over 60% of the total fluorescence change associated with refolding occurs during the 2-ms dead time of the stopped-flow measurement (cf. Figure 6). This burst-phase intermediate is destabilized with increasing GuHCl concentration and is no longer populated in the unfolding transition region. The sigmoid character of the initial amplitude as a function of GuHCl concentration suggests that the burst-phase intermediate represents a well-defined state that undergoes a cooperative unfolding transition in the range from 1 to 2 M GuHCl. The low fluorescence intensity, approaching that of the native state at low GuHCl concentrations, is indicative of a condensed state with Trp 45 partially buried in an apolar environment. In contrast to these measurements at 25 °C, the stopped-flow results at 8 °C show no indication for folding intermediates, in terms of both rates and amplitudes (Figure 8). The destabilization of the burst-phase intermediate at low temperature supports our conclusion that it is a collapsed

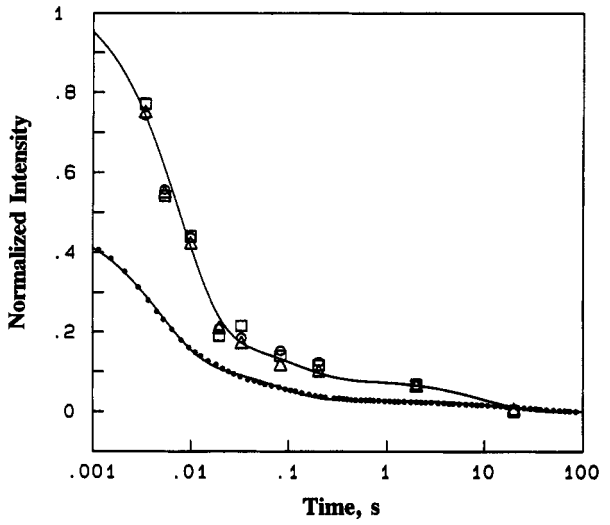

FIGURE 9: Comparison of the WT and F45W refolding kinetics under matching conditions (1 M GuHCl, pH 5.0, and 25 °C). The top curve represents the folding kinetics of WT ubiquitin monitored by pulsed hydrogen exchange (Briggs & Roder, 1992) for representative amide protons in the α-helix (V26, □), the β-sheet (V5, ○), and the helix–sheet interface (I23, △). The bottom trace is the fluorescence-detected refolding kinetics of F45W normalized to the fluorescence of the unfolded protein extrapolated to 1 M GuHCl (cf. Figure 7).

state stabilized primarily by hydrophobic interactions, which are known to be weakened at low temperature (Kauzman, 1959; Privalov, 1979).

Burst-phase intermediates have been described for a number of proteins, primarily on the basis of kinetic CD observations on early folding intermediates with substantial amounts of secondary structure [reviewed by Kuwajima (1989); more recent reports include Kuwajima et al. (1991), Elöve et al. (1992), and Radford et al. (1992)]. However, such early folding events have only rarely been observed by other probes. In recent folding studies on cytochrome *c*, Elöve et al. (1992) detected rapid changes on the millisecond time scale not only in the far-UV region of the CD spectrum but also by fluorescence, indicating the formation of a compact intermediate in which the fluorescence of a single tryptophan, Trp 59, is partially quenched by the heme group. Other reports of rapid chain condensation events are based on kinetic ANS binding studies (Ptitsyn et al., 1990; Semisotnov et al., 1991).

Since we have been unable to monitor the folding reaction of WT ubiquitin with optical probes (near-UV absorbance and tyrosine fluorescence), we relied on the much more time-consuming pulsed hydrogen-exchange method for kinetic folding studies (Briggs & Roder, 1992). In Figure 9, we compare the fluorescence results on F45W from this study (Figure 6) with the time course of amide protection from our previous pulsed hydrogen-exchange study on the wild type (Briggs & Roder, 1992) under the same refolding conditions (1 M GuHCl, pH 5, 25 °C). Both experiments show a major folding phase with a time constant of 5–10 ms, as well as two minor phases with time constants of about 100 ms and 10 s, respectively. However, there is no evidence for any rapid protection of amide protons during the dead time (~5 ms) of the quenched-flow experiment, in contrast to the fluorescence-detected folding kinetics which shows about 50% burst phase under these conditions. Apparently, a cluster of hydrophobic residues involving Trp 45 is already assembled within the first few milliseconds of folding, but the structure formed does not protect amide protons against hydrogen exchange. Amide protection indicative of the formation of stable hydrogen-bonded structure is only observed in a major folding event on the 10-ms time scale (Briggs & Roder, 1992). The comparison of kinetic CD and pulsed hydrogen-exchange results on cytochrome *c* (Elöve et al., 1992) and lysozyme (Radford et al., 1992) has led to similar conclusions.

Conclusions. We have shown that mutation of Phe 45 to Trp results in a biologically active ubiquitin variant with minor structural perturbations and only slightly reduced structural stability. The presence of an interior tryptophan side chain provides a sensitive conformational probe for thermodynamic and kinetic folding studies. Systematic fluorescence studies of the kinetics of folding and unfolding as a function of denaturant concentration and temperature revealed a partly condensed early folding intermediate in which Trp 45 is largely shielded from the solvent. The tryptophan-containing variant of ubiquitin now serves as the starting point for further studies on the effect of amino acid changes on ubiquitin stability and folding.

ACKNOWLEDGMENT

We thank Dr. A. L. Haas and T. Burch for performing some of the assays of ubiquitin function, Dr. S. Luck for the development of a data acquisition program, P. Laub for assistance in structural analysis, J. M. Sauder and Y. Zhang for help with 2D NMR, and Drs. G. A. Elöve, M. Gochin, and E. K. Jaffe for critical reading and suggestions.

REFERENCES

Alexander, P., Fahnestock, S., Lee, T., Orban, J., & Bryan, P. (1992) *Biochemistry 31*, 3597–3603.
Anil-Kumar, Ernst, R. R., & Wüthrich, K. (1980) *Biochem. Biophys. Res. Commun. 95*, 1–6.
Baldwin, R. L., & Roder, H. (1991) *Curr. Biol. 1*, 218–220.
Baum, J., Dobson, C. M., Evans, P. A., & Hanley, C. (1989) *Biochemistry 28*, 7–13.
Bax, A., & Davis, D. G. (1985) *J. Magn. Reson. 65*, 355–360.
Beasty, A. M., Hurle, M. R., Manz, J. T., Stackhouse, T., Onuffer, J. J., & Matthews, C. R. (1986) *Biochemistry 25*, 2965–2974.
Braunschweiler, L., & Ernst, R. R. (1983) *J. Magn. Reson. 53*, 521–528.
Briggs, M. S., & Roder, H. (1992) *Proc. Natl. Acad. Sci. U.S.A. 89*, 2017–2021.
Ciechanover, A., Hod, Y., & Hershko, A. (1978) *Biochem. Biophys. Res. Commun. 81*, 1100–1105.
Ciechanover, A., Elias, S., Heller, H., Ferber, S., & Hershko, A. (1980) *J. Biol. Chem. 255*, 7525–7528.
Creighton, T. E. (1990) *Biochem. J. 270*, 1–16.
Di Stefano, D. L., & Wand, A. J. (1987) *Biochemistry 26*, 7272–7281.
Ecker, D. J., Butt, T. R., Marsh, J., Sternberg, E. J., Morgolis, N., Monia, B. P., Jonnalagadda, S., Kahn, M. I., Weber, P. L., Mueller, L., & Crooke, S. T. (1987a) *J. Biol. Chem. 262*, 14213–14221.
Ecker, D. J., Khan, M. I., Marsh, J., Butt, T. R., & Crooke, S. T. (1987b) *J. Biol. Chem. 262*, 3524–3527.
Elöve, G. A., Chaffotte, A. F., Roder, H., & Goldberg, M. E. (1992) *Biochemistry 31*, 6876–6883.
Gill, S. C., & von Hippel, P. H. (1989) *Anal. Biochem. 189*, 319–326.
Goldenberg, D. P., Frieden, R. W., Haack, J. A., & Morrison, T. B. (1989) *Nature 338*, 127–132.
Haas, A. L., & Rose, I. A. (1982) *J. Biol. Chem. 257*, 10329–10337.

Hershko, A., Heller, H., Elias, S., & Ciechanover, A. (1983) *J. Biol. Chem. 258*, 8206–8214.
Hughson, F. M., Wright, P. E., & Baldwin, R. L. (1990) *Science 249*, 1544–1548.
Ikeguchi, M., Kuwajima, K., Mitani, M., & Sugai, S. (1986) *Biochemistry 25*, 6965–6972.
Jackson, S. E., & Fersht, A. R. (1991) *Biochemistry 30*, 10428–10435.
Jeng, M.-F., Englander, S. W., Elöve, G. A., Wand, A. J., & Roder, H. (1990) *Biochemistry 29*, 10433–10437.
Jensen, J., Goldstein, G., & Breslow, E. (1980) *Biochim. Biophys. Acta 624*, 378–385.
Kauzmann, W. (1959) *Adv. Protein Chem. 14*, 1–63.
Kim, P. S., & Baldwin, R. L. (1990) *Annu. Rev. Biochem. 59*, 631–660.
Kuwajima, K. (1989) *Proteins: Struct., Funct., Genet. 6*, 87–103.
Kuwajima, K., Garvey, E. P., Finn, B. E., Matthews, C. R., & Sugai, S. (1991) *Biochemistry 30*, 7693–7703.
Lenkinsiki, R. E., Chen, D. M., Glickson, J. D., & Goldstein, G. (1977) *Biochim. Biophys. Acta 494*, 126–130.
Macura, S., & Ernst, R. R. (1980) *Mol. Phys. 41*, 95–117.
Marion, D., & Wüthrich, K. (1983) *Biochem. Biophys. Res. Commun. 113*, 967–974.
Matouschek, A., Kellis, J. T., Jr., Serrano, L., Bycroft, M., & Fersht, A. R. (1990) *Nature 346*, 440–445.
Matouschek, A., Serrano, L., & Fersht, A. R. (1992) *J. Mol. Biol. 224*, 819–835.
Matthews, C. R. (1987) *Methods Enzymol. 154*, 498–511.
Matthews, C. R. (1991) *Curr. Opin. Struct. Biol. 1*, 28–35.
Pace, C. N. (1986) *Methods Enzymol. 131*, 266–280.
Pace, C. N., Laurents, D. V., & Erickson, R. E. (1992) *Biochemistry 31*, 2728–2734.
Privalov, P. L. (1979) *Adv. Protein Chem. 33*, 167–241.
Ptitsyn, O. B. (1987) *J. Protein Chem. 6*, 273–293.
Ptitsyn, O. B., Pain, R. H., Semisotnov, G. V., Zerovnik, E., & Razgulyaev, O. I. (1990) *FEBS Lett. 262*, 20–24.
Radford, S. E., Dobson, C. M., & Evans, P. A. (1992) *Nature 358*, 302–307.
Rance, M., Wagner, G., Sorensen, O. W., Wüthrich, K., & Ernst, R. R. (1984) *J. Magn. Reson. 59*, 250–261.
Roder, H. (1989) *Methods Enzymol. 176*, 446–473.
Roder, H., & Elöve, G. A. (1993) In *Frontiers in Molecular Biology*, in press.
Roder, H., Elöve, G. A., & Englander, S. W. (1988) *Nature 335*, 700–704.
Semisotnov, G. V., Rodionova, N. A., Razgulyaev, O. I., Uversky, V. N., Gripas, A. F., & Gilmanshin, R. I. (1991) *Biopolymers 31*, 119–128.
Shaka, A. J., & Freeman, R. (1983) *J. Magn. Reson. 51*, 169–173.
Stryer, L. (1968) *Science 162*, 526–533.
Tanford, C. (1968) *Adv. Protein Chem. 23*, 121–282.
Tanford, C. (1970) *Adv. Protein Chem. 24*, 1–95.
Udgaonkar, J. B., & Baldwin, R. L. (1988) *Nature 335*, 694–699.
Vijay-Kumar, S., Bugg, C. E., & Cook, W. J. (1987) *J. Mol. Biol. 194*, 531–544.
Weber, P. L., Brown, S. C., & Mueller, L. (1987) *Biochemistry 26*, 7282–7290.
Weber, P. L., Ecker, D. J., Marsh, J., Crooke, S. T., & Mueller, L. (1988) *Trans. Am. Crystallogr. Assoc. 24*, 91–105.
Wood, L. C., White, T. B., & Nall, B. T. (1988) *Biochemistry 27*, 8562–8568.
Wöstmann, C., Tannich, E., & Bakker-Grunwald, T. (1992) *FEBS Lett. 308*, 54–58.
Wüthrich, K., Roder, H., & Wagner, G. (1980) In *Protein Folding* (R. Jaenicke, Ed.) pp 549–564, Elsevier/North-Holland, Amsterdam.